

# PCCP

Accepted Manuscript



This is an *Accepted Manuscript*, which has been through the Royal Society of Chemistry peer review process and has been accepted for publication.

*Accepted Manuscripts* are published online shortly after acceptance, before technical editing, formatting and proof reading. Using this free service, authors can make their results available to the community, in citable form, before we publish the edited article. We will replace this *Accepted Manuscript* with the edited and formatted *Advance Article* as soon as it is available.

You can find more information about *Accepted Manuscripts* in the [Information for Authors](#).

Please note that technical editing may introduce minor changes to the text and/or graphics, which may alter content. The journal's standard [Terms & Conditions](#) and the [Ethical guidelines](#) still apply. In no event shall the Royal Society of Chemistry be held responsible for any errors or omissions in this *Accepted Manuscript* or any consequences arising from the use of any information it contains.

# Dual Descriptor and Molecular Electrostatic Potential: Complementary Tools for the Study of the Coordination Chemistry of Ambiphilic Ligands

Frédéric Guégan,<sup>\*,†</sup> Pierre Mignon,<sup>†</sup> Vincent Tognetti,<sup>‡</sup> Laurent Joubert,<sup>‡</sup> and  
Christophe Morell<sup>\*,†</sup>

*Laboratoire des Sciences Analytiques, UMR CNRS 5280, Université Claude Bernard Lyon 1 69622 Villeurbanne Cedex, FRANCE, and Normandy University, COBRA UMR 6014 & FR 3038, Université de Rouen, INSA Rouen, CNRS, 1 rue Tesnière 76821 Mont St Aignan, Cedex, FRANCE*

E-mail: frederic.guegan@ens-lyon.org; christophe.morell@univ-lyon1.fr

---

\*To whom correspondence should be addressed

<sup>†</sup>Laboratoire des Sciences Analytiques, UMR CNRS 5280, Université Claude Bernard Lyon 1 69622 Villeurbanne Cedex, FRANCE

<sup>‡</sup>Normandy University, COBRA UMR 6014 & FR 3038, Université de Rouen, INSA Rouen, CNRS, 1 rue Tesnière 76821 Mont St Aignan, Cedex, FRANCE

### Abstract

In this paper, we show that the ambiphilic properties of some organic ligands in organometallic complexes may be retrieved readily from simple calculations in the framework of Conceptual Density Functional Theory (C-DFT). Namely, the dual descriptor (DD) and the molecular electrostatic potential (MEP) of the ligands afford a rather straightforward interpretation of experimental trends such as the bonding geometry and the electronic properties of complexes in terms of  $\sigma$ -,  $\pi$ - and back-bonding. The studied ligands were chosen to be representative of the wide variety organometallic chemistry offers, ranging from neutral to charged systems and from diatomic to polyatomic molecules. The present approach is general since all relevant parameters are retrieved from the electron density, obtained either from a DFT or post-Hartree Fock calculation. It is believed to be helpful for organometallic chemists, since it allows a deep understanding and may be used as a predictive tool of the coordinating properties of ligands.

## 1-Introduction

The interplay between metallic cation(s) and organic ligand(s) is the cornerstone of organometallic chemistry<sup>1</sup>. According to the simplest scheme, the metallic cations are perfect Lewis acids and the ligands, perfect Lewis bases<sup>2</sup>. However, these ideal cases are certainly not the most interesting from the theoretical and practical point of view. Indeed, most of the time, ligands can also be electrophilic and metals may display a nucleophilic character. This results in non-obvious situations where electron transfers may occur either from ligand to metal and the other way around (as involved for instance in the Dewar-Chatt-Duncanson model<sup>3</sup>). As a consequence, charge transfers are likely to occur, and, in the end, coordination bonds are intermediates between purely ionic and purely covalent. The limits of the so-called Klopman-Salem model<sup>4,5</sup>, stating that reactions usually imply either a charge or an orbital control, are in these cases reached. Hence, to get a complete picture of the chemical behaviour of organometallic compounds one has to rely upon two descriptors, one of them characterizing the charge transfer while the other should describe the electrostatic interactions.

Within the canonical ensemble, such descriptors can be deduced from a survey of the variations of the total energy when the molecule reacts with another compound. To do so, we can perform a second order Taylor expansion of the variations of the total molecular energy with respect to the variation of the external potential  $\delta v(\mathbf{r})$  and the number of electrons  $dN$ :

$$dE[v(\mathbf{r}); N] = \mu dN + \frac{\eta}{2} dN^2 + dE_{NN} + \int \rho(\mathbf{r}) \delta v(\mathbf{r}) d^3\mathbf{r} + dN \int f(\mathbf{r}) \delta v(\mathbf{r}) d^3\mathbf{r} + \frac{1}{2} \iint \chi(\mathbf{r}, \mathbf{r}') \delta v(\mathbf{r}) \delta v(\mathbf{r}') d^3\mathbf{r} d^3\mathbf{r}' \quad (1)$$

with  $E_{NN}$  the nuclei-nuclei repulsion energy,  $\mu$  the electronic chemical potential,  $\eta$  the molecular hardness,  $f(\mathbf{r})$  the Fukui function and  $\chi(\mathbf{r}, \mathbf{r}')$  the non-local linear response kernel (whose evaluation is rather cumbersome and will not be considered in this study). The two first contributions on the right-hand side of equation 1 are global properties which describe the general response of the molecule as a whole. Conversely, the other terms are essentially



local and bear informations on the possible regioselectivity of the process, which is the main target of our study. These local terms can be merged in two groups, the first contribution being:

$$dE_1 = dE_{NN} + \int \rho(\mathbf{r}) \delta v(\mathbf{r}) d^3\mathbf{r} \quad (2)$$

$$= \int \left( - \sum_M Z_M \delta_D(\mathbf{r} - \mathbf{R}_M) + \rho(\mathbf{r}) \right) \delta v(\mathbf{r}) d^3\mathbf{r} \quad (3)$$

for a system composed of  $M$  atoms of atomic charges  $Z_M$ , located at  $\mathbf{R}_M$  positions (and  $\delta_D$  being the Dirac distribution). It is plain to see that this term will essentially contain the electrostatic contributions to the energy variation, plus an exchange and correlation contribution. However, knowing that electrostatic effects are usually more long-ranged than exchange and correlation ones for a charged species, if we assume that our reaction implies ions which are quite remote from each other (early stages of the reaction) the incoming reactant can be treated to a first approximation as a point charge, placed at  $\mathbf{R}_{pc}$ . The variations of the external potential will thus be approximated by:

$$\delta v(\mathbf{r}) = \frac{\delta q}{|\mathbf{r} - \mathbf{R}_{pc}|} \quad (4)$$

Putting equation 4 in equation 3 yields:

$$dE_1 = \delta q \left( \sum_M Z_M \int \frac{\delta_D(\mathbf{r} - \mathbf{R}_M)}{|\mathbf{r} - \mathbf{R}_{pc}|} d^3\mathbf{r} - \int \frac{\rho(\mathbf{r})}{|\mathbf{r} - \mathbf{R}_{pc}|} d^3\mathbf{r} \right) \quad (5)$$

$$= \delta q \left( \sum_M \frac{Z_M}{|\mathbf{R}_M - \mathbf{R}_{pc}|} - \int \frac{\rho(\mathbf{r})}{|\mathbf{r} - \mathbf{R}_{pc}|} d^3\mathbf{r} \right) = \delta q \cdot MEP(\mathbf{R}_{pc}) \quad (6)$$

where MEP is the molecular electrostatic potential. As a result, this first local term seems to fit for description of chemical properties driven by charge interactions.

On the other hand, the second term of equation Eq. (1):

$$dE_2 = dN \int f(\mathbf{r}) \delta v(\mathbf{r}) d^3\mathbf{r} \quad (7)$$

involves the Fukui function, which is defined as

$$f(\mathbf{r}) = \left( \frac{\partial \rho(\mathbf{r})}{\partial N} \right)_{v(\mathbf{r})} \quad (8)$$

Actually, because of the discontinuity of the energy derivatives with respect to the number of electrons, one should rather consider the left ( $\Delta N < 0$ ) and right ( $\Delta N > 0$ ) derivatives, respectively corresponding to the  $f^-(\mathbf{r})$  and  $f^+(\mathbf{r})$  Fukui functions. From their definitions, it is obvious that  $f^+(\mathbf{r})$  allows to find the electrophilic regions, which are likely to gain electrons ( $\Delta N > 0$ ), and  $f^-(\mathbf{r})$  is more fit for looking to the nucleophilic regions (which are prone to lose electron density). This suggests  $dE_2$  would be rather adapted to describe chemical properties that are driven by "orbital" interactions, or more properly by charge densities interactions (between nucleophilic and electrophilic regions). As a result, the two local contributions  $dE_1$  and  $dE_2$  should reveal complementary to study ambiphilic ligands, in the spirit of an extended Klopman-Salem model (where one considers both electrostatic and "orbital" contribution). A further step can be done by replacing the two Fukui functions by a single descriptor, the dual descriptor (DD)<sup>6,7</sup>:

$$\Delta f(\mathbf{r}) = \left( \frac{\partial^2 \rho(\mathbf{r})}{\partial N^2} \right)_{v(\mathbf{r})} \quad (9)$$

It has indeed been shown that this descriptor also conveys information about the charge densities interaction. More specifically, one has  $\Delta f(\mathbf{r}) > 0$  wherever the molecule is likely to receive electron density (electrophilic regions) and  $\Delta f(\mathbf{r}) < 0$  wherever the density is likely to escape (nucleophilic regions).

As a consequence, the combination of the MEP and the DD seems adapted to study

the coordination chemistry of organometallic complexes. A further simplification of the problem can still be made, considering that usually experimentalists focus on the ligand properties rather than on the metal properties. This is likely due to the fact that changing the metal results in dramatic changes in chemical behaviour, while the synthetic variations of the ligand, such as pendant arms or donor acceptor substituent, lead to more subtle adjustments. The problem at hand is therefore reduced to a proper description of the ligand properties. They must be characterized at both a global and local level, that is to say being able to ascertain whether the ligand is rather nucleophilic, electrophilic or both, and its regioselectivity or regiospecificity.

So, in line with recently published studies<sup>8-10</sup>, we propose to use a combination of the DD and the MEP to explain the coordination abilities of ambiphilic or potentially ambiphilic ligands towards metallic cations. To do so, the needed equations are recalled in section 2, where the details of the computation of the two descriptors are also given. An emphasis is made on the decomposition of the dual descriptor, which allows to quantify and to build a scale of electrophilicity/nucleophilicity for the studied ligands. In section 3, different examples are shown and analysed, with a special emphasis on the rationalisation of the experimental trends. Noticeably, ambiphilic behaviours are explicitly rationalised in terms of electron density ("orbital") and charge interactions. Finally, the paper ends with some concluding remarks.

## 2-Theoretical and computational details

### State Specific and usual Dual Descriptor

As discussed in the introduction, calculation of both the MEP and the DD for different ligands should allow us to map quite efficiently their reactivity. Most of computational software now include direct calculations of molecular electrostatic properties (up to the hexapole moment). However it is not necessarily the case for the dual descriptor. Furthermore, equation

Eq. (9) is not readily applicable and thus needs to be developed. Usually, two layers of approximations are used<sup>11</sup>:

- Finite difference approximation: one usually approximate the derivative in equation Eq. (9) by the finite variations of the density upon addition or subtraction of electrons.

This yields:

$$\Delta f(\mathbf{r}) \approx \left( \frac{\rho_{N+1}(\mathbf{r}) - \rho_N(\mathbf{r})}{(N+1) - (N)} - \frac{\rho_N(\mathbf{r}) - \rho_{N-1}(\mathbf{r})}{(N) - (N-1)} \right) = \rho_{N+1}(\mathbf{r}) + \rho_{N-1}(\mathbf{r}) - 2\rho_N(\mathbf{r}) \quad (10)$$

where  $\rho_{N\pm i}(\mathbf{r})$  represents the electron density of the system under addition or subtraction of one electron, at constant geometry.

- Frozen orbital hypothesis: if the orbitals remain unchanged upon addition and subtraction of one electron, the only non zero contribution in the previous difference arises from the frontier orbitals. By identification of the two fractions in expression Eq. (10), one gets:

$$\Delta f(\mathbf{r}) \approx \rho_{LU}(\mathbf{r}) - \rho_{HO}(\mathbf{r}) \quad (11)$$

with  $\rho_{LU}(\mathbf{r})$  and  $\rho_{HO}(\mathbf{r})$  are the densities of the LUMO and HOMO obtained in a SCF calculation on the system with N electrons.

Some problems arise with these formulations. First, regardless of the frozen orbital hypothesis, equation Eq. (11) suffers from severe limitations: when considering a highly correlated system, canonical orbitals do not convey any relevant information, or when either the LUMO or HOMO show some degeneracy, this equation becomes quite meaningless. Moreover, when the studied compounds are already negatively charged, the addition of one electron (as done in equation Eq. (10)) might also not be plain. The possible self-ionisation would be missed because of the restricted size of the basis set (the additional electron being localised on an unphysical state). These formulations are also not well formulated for open-shell systems, where the resulting spin state after addition or subtraction of one electron is not obvious. A

powerful formulation was recently proposed by some of the authors, and seems well suited for this kind of study: the state specific dual descriptor<sup>12</sup>. In this formulation, the dual descriptor is calculated as the variations in electron density between the excited states and the ground state:

$$\Delta f_{(i)}(\mathbf{r}) = \rho_{(i)}(\mathbf{r}) - \rho_{(0)}(\mathbf{r}) \quad (12)$$

with  $\rho_{(i)}(\mathbf{r})$  the density of the excited state  $i$  ( $i=0$  meaning ground state). The physical meaning of this development is quite simple: as two reagents approach one another, they exert a mutual perturbation on their densities, through a variation of the external potential. As a result, the perturbed density of a molecule in this reacting configuration is markedly different from the ground state density of the isolated molecule. Assuming that no geometric relaxation occurs - i.e., that the variation of the external potential is only due to the approach of the other reagent - this perturbation can be developed on the basis of all the excited states of the isolated molecule. In other words, the approach of a reagent changes the external potential in such a way that excited states can be stabilised, hence yielding a more accurate representation of the properties of the reacting molecule than what the isolated ground state configuration would.

Ideally one should sum up the  $\Delta f_{(i)}$  contributions of all the excited states into the so-called extended DD, with a weighting as all the states will not contribute in the same way to the reactivity. The fact is that this weighting remains unknown, but one can assume reasonably that the higher in energy a state is, the less it will contribute to the reactivity in the ground state, as exemplified by the sum-over-states formula giving the molecular polarisability<sup>13</sup>. As a rule of thumb, one might quite often rely upon the very first excited states (first or second), and resume the extended DD to the corresponding state-specific DD<sup>14</sup>.

## Description by domains and quantification

Since the DD sums to 0 over the molecule (by construction of the DD), both electrophilic and nucleophilic sites should be present on a given reagent, and there is no reason for an atom to show only one of the two behaviours. In fact, it will be shown hereafter that atoms quite generally exhibit both contributions. However, caution must be taken if one wants to compare the electrophilic and nucleophilic contributions between different ligands. The "crude" numerical values can indeed only be compared between systems with the same number of electrons. One can relieve this condition by moving from the canonical to the grand canonical ensemble<sup>15</sup>; upon the Legendre transform  $E \rightarrow \Omega = E - \mu N$  (with  $\mu$  the electronic chemical potential) one can define a grand-canonical dual descriptor:

$$\left( \frac{\partial^2 \rho(\mathbf{r})}{\partial \mu^2} \right)_{v(\mathbf{r})} = \frac{\Delta f(\mathbf{r})}{\eta^2} - \frac{\gamma}{\eta^3} f(\mathbf{r}) \quad (13)$$

with  $\eta$  and  $\gamma$  being respectively the chemical hardness and hyperhardness, and  $f(\mathbf{r})$  being the Fukui function. The last term of equation Eq. (13) can quite reasonably be neglected, since the ratio  $\gamma/\eta^3$  is generally quite small, even though hyperhardness is not necessarily close to zero, unlike what is generally assumed<sup>16</sup>. Hence, in the following we will restrict to the computation of the first term  $\Delta f(r)/\eta^2$ ,  $\Delta f(r)$  being computed through the first state specific (canonical) dual descriptor.

Another step must be taken if one wants to compare the chemical properties of different ligands. The grand canonical DD is indeed a local function. Yet, usually reactivity in chemistry is discussed in terms of reactive sites, thus using a "coarse-grained" description of the reaction. One must then translate local properties into atomic or fragment contributions. This approach is called condensation, the most widespread being the one developed by Yang and Mortier<sup>17</sup>, based on atomic charges  $q(A)$  (whatever their definition). For instance, the

condensed values of the Fukui functions are:

$$f^{\pm}(A) = \mp [q_N(A) - q_{N\pm 1}(A)] \quad (14)$$

with  $q_{N\pm 1}(A)$  the charge of an atom A when an electron is added or withdrawn to the molecule through a vertical process (no geometrical rearrangement). The extension to the state-specific dual descriptor is quite straightforward:

$$\Delta f_i(A) = q_{GS}(A) - q_{ESi}(A) \quad (15)$$

where  $q_{GS}(A)$  is the charge of A in the ground state and  $q_{ESi}(A)$  the charge in the  $i$ th excited-state. Albeit very useful, such a scheme presents some severe drawbacks. Consider for instance a homodiatom molecule  $A_2$ . By symmetry,  $q_{N\pm 1}(A) = \mp \frac{1}{2}$ , which yields:

$$\forall A, f^{\pm}(A) = \frac{1}{2}, \Delta f(A) = 0. \quad (16)$$

In other words, such a scheme is unable to distinguish between  $H_2$ ,  $O_2$ ,  $N_2$  and  $F_2$  for instance, whereas their reactivity strongly differ as it will be shown in the next section.

We recently devised a new approach able to discriminate between such molecules. The real space is divided into non-overlapping domains  $D_i$  of constant sign for the DD. In practice, from a DD Cartesian grid (cube file), a given grid point is said to belong to the interior of one and only one domain if the DD takes the same sign at every neighbouring points. Refinements were also implemented in order to assure the robustness of this assignment and the stability of such a grid-based algorithm. Once these domains are obtained, the corresponding condensed values are defined by:

$$\Delta f(D_i) = \int_{D_i} \Delta f(\mathbf{r}) d^3\mathbf{r} \quad (17)$$

These integrals are computed numerically on the Cartesian grid. In order to assess the accuracy of such a procedure, one should monitor that:

$$\sum_i \Delta f(D_i) \approx 0 \quad (18)$$

As an even more coarsened-grained representation, the following descriptors can also be evaluated:

$$\Delta f_D^+ = \sum_{i/f(D_i)>0} \Delta f(D_i) \quad (19)$$

$$\Delta f_D^- = \sum_{i/f(D_i)<0} \Delta f(D_i) \quad (20)$$

which measure the overall predominant electrophilic and nucleophilic propensities. Note that the DD normalisation implies that  $\Delta f_D^+ = -\Delta f_D^-$ . It is also worth adding that from this partition, other domain properties could be evaluated such as populations, barycentres, moments... Their computation and their use will be described in a forthcoming paper.

## Computational details

All ligands structures presented in table Table 3 were fully optimised without symmetry restriction at the DFT level of theory. All calculations were carried out using the hybrid B3LYP functional, and the 6-31G\* gaussian basis set except for the thiocyanate anion and the dihalogens. SCN<sup>-</sup> anion was optimised using the 6-31+G\* basis set, as previous studies stressed the need to use diffuse functions to properly model sulfur atoms<sup>18,19</sup>. Dihalogens were optimised using the full-electron, double-zeta with polarisation functions DGDZVP basis set<sup>20</sup>, to ensure consistency of the results and since iodine is unavailable in the 6-31G\* basis set. Frequency calculations were performed at the same level of theory to check for no imaginary value. Then, the first ten excited states were computed in the framework of Time Dependent DFT (TD-B3LYP). Subsequently, the DD was computed according to equation



Eq. (12), using the densities of either the first excited states.

Grand canonical DDs (approximated by their first state-specific components) were represented as isosurfaces, and MEP obtained from the ground state calculations were mapped on density isosurfaces ( $1.10^{-3}$  a.u.), using GaussView 5<sup>21</sup>. Chemical hardness was simply computed as the energy difference  $\eta \approx E_{LUMO} - E_{HOMO}$ . When relevant, condensations of the DD were computed according to the former scheme (equation 19-20) in order to relieve ambiguities or add a supplementary level of explanation to the discussion.

All calculations were carried out using the Gaussian09 code and utilities<sup>22</sup>. Condensations were made using a home made program.

### 3-Discussion

Various systems were studied here, merged as shown in the series listed in table Table 3. The groups were assembled according to the similarities of the ligands reactivity - as H<sub>2</sub> and ethene for instance - or to the number of electrons - as for series (4). Results are discussed hereafter.

#### Series (1): H<sub>2</sub> and ethene

Ethene and dihydrogen usually show a similar reactivity as ligands, since they both interact by their main bond, coordinating in a  $\eta^2$  mode<sup>1</sup> (*cf.* scheme Scheme 1(a)). Therefore, it seemed rather logical to compare their features at the DD and MEP level, represented in figure Figure 1. As formerly said, one can see that both nucleophilic and electrophilic parts are observed on the same atoms. The nucleophilic area is indeed located on both sides of the bond (H-H or C=C), indicating a coordination promoted by these bonds. MEP surfaces indicate the same coordination mode, since negative potential surfaces (stabilising for a cation) are found on the sides of the main bonds. In the case of H<sub>2</sub>, the minimal value is small (*ca.*  $-3.10^{-3}$  a.u.) and the attractive domain quite narrow, which suggests a quite

weak bonding. In the case of ethene, the minimal value for the potential is one order of magnitude larger (*ca.*  $3.10^{-2}$  a.u.) and the attractive domains are larger in space, hence implying a stronger bonding capability for ethene as compared to  $H_2$ . This is consistent with the known geometries and relative stability of hydrogen and ethene complexes, for instance  $[W(P^iPr)_2(CO)_3(H_2)]$  and Zeise's salt<sup>1</sup>  $[PtCl_3(C_2H_4)]^-$ . Furthermore, electrophilic systems are found, pointing outward the molecule, essentially  $\pi^*$  or  $\sigma^*$ -like (in the framework of MO theory<sup>23</sup>). They develop in the neighbourhood of the coordinating site, suggesting a quite efficient backbonding. This is in perfect line with experimental results on ethylene-based complexes, such as tris-ethylene nickel(0)<sup>24</sup> where a quite efficient back-bonding is seen. The reactivity of  $H_2$  is also well reproduced, as seen for instance in the oxidative addition of  $H_2$  on Vaska's complex<sup>25</sup>  $[IrCl(CO)(PPH_3)_2]$ , or the relative difficulty to ascertain the oxidation state of the hydrogens in  $H_2$  based complexes, between di-hydrido and neutral dihydrogen<sup>26</sup>.

## Series (2): dihalogens

Isosurfaces in the case of the dihalogens from  $F_2$  to  $I_2$  are represented in figure Figure 2. Here, caution must be taken when using the term ligand. Indeed, as Rogachev and Hoffmann already stressed previously<sup>27</sup> (and references therein), despite the lone pairs that should turn dihalogens into very good ligands, only a few transition metal complexes involving iodine are known<sup>28-31</sup>, and to the best our knowledge, none involving other halogens.

Nevertheless, it seemed rather logical to investigate not only iodine, but also lighter parent compounds, and to check if any disparity could be found. The general trends are globally the same, for the first two excited states (they are degenerated, and give the same results). All compounds show electrophilicity along the molecular axis, essentially  $\sigma^*$ -like (in the framework of MO theory), while nucleophilic areas point on both sides of the bond where one would expect to find lone pairs. These features are consistent with the aforementioned study, where iodine is considered to be essentially electrophilic while coordinating in a linear

fashion, and nucleophilic when coordinating on a "bent-side on" mode. The MEP is also in a quite good agreement, developing negative contribution on the sides of the molecules where the nucleophilic lobes are located, and positive (repulsive) contributions along the molecular axes. These electrophilic and positive MEP areas represent general features of halogen compounds, the so-called  $\sigma$ -holes<sup>32</sup>. The bent-side on coordination seems therefore plausible, and is more probable for the heavier halogens since both the minimal values and extents of the attractive MEP domains are larger (from ca.  $-3.10^{-3}$  a.u. for  $F_2$  to  $-7.10^{-3}$  a.u. for  $I_2$  and  $Br_2$ ). The larger proclivity of the heaviest halogens towards coordination is also stressed by the increase in the spatial extent of the nucleophilic parts of the DD as one moves from fluorine to iodine. It is likewise found in the condensed values of the DD, as shown in table Table 1. As a remark, it is worth noticing that the condensation scheme respects the condition of a zero integral of the DD (equation Eq. (18)).

Table 1: Condensed grand canonical dual descriptor for the dihalogens, sorted by positive or negative contribution.

Molecule	$\Delta f_D^+/\eta^2$ (a.u)	$\Delta f_D^-/\eta^2$ (a.u)
$F_2$	9.50	-9.50
$Cl_2$	21.36	-21.40
$Br_2$	32.86	-32.97
$I_2$	48.06	-48.42

It is plain to see that nucleophilic contributions are increasing when moving from fluorine to iodine, suggesting a more efficient coordination for heavier dihalogens. Both this tendency and the topological features of the DD account for the coordination geometry of iodine<sup>31</sup> in  $[Rh(CF_3CO_2)_4(I_2)]$ , and two more factors might play a role for the non existence of other donor dihalogen complexes. First, the weak electrostatic stabilisation (for chlorine and fluorine) can be insufficient to allow a cation approach. Furthermore, dihalogens are quite strong oxidants, hence suggesting that the complexes they might form would not be stable and would undergo oxidative addition with a cleavage of the halogen-halogen bond. This tendency would be exacerbated for the first dihalogens, which show the highest redox potentials (we recall here the standard potentials:  $E^0(F_2/F^-) = 2.866$  V/ECS,  $E^0(Cl_2/Cl^-)$

= 1.358 V/ECS,  $E^0(\text{Br}_2/\text{Br}^-) = 1.087$  V/ECS versus  $E^0(\text{I}_2/\text{I}^-) = 0.536$  V/ECS<sup>33</sup>. This hypothesis is supported by the reactivity of  $[(\text{dpp}-\text{nacnac}^{\text{CH}_3})\text{Rh}(\text{phdi})]$  towards dihalogens<sup>29</sup>. Indeed, addition of chlorine or bromine to this complex leads to an oxidation of the metal center and a cleavage of the halogen-halogen bond, while addition of iodine does not. In this case, a linear-acceptor iodine ligand is found, which is consistent with the description obtained by the DD. The supposed mechanism is depicted on scheme Scheme 1 (b). Actually, two other linear-acceptor iodine based complexes are known<sup>28,30</sup>:  $[\text{Pt}(\text{dmpe})_2(\text{I}_2)]$  and  $[\text{PtI}(\text{C}_6\text{H}_3(\text{CH}_2\text{NMe}_2)_2)(\text{I}_2)]$ . This small number of examples seems to agree well with the previous discussion about the redox activity and both the smaller developments of the DD for lighter halogens, and another feature may explain the relative rarity of complexes based on acceptor iodine. It is indeed plain to see that the linear coordination is electrostatically disfavoured, since the MEP displays along the molecular axis of the dihalogens its largest value, *ca.* 0.022, 0.038, 0.049, 0.052 a.u. from  $\text{F}_2$  to  $\text{I}_2$ .

As a result, one can see that coordination abilities of dihalogens are quite similar according to the DD and the MEP analyses. Both show a tendency towards donation in a bent-side on geometry, which is expected to be favoured only for the heavier dihalogens. An acceptor ability in a linear coordination geometry is also found, which is expected to be also quite effective for the heavier halogens since they display a smaller gap between their HOMO and LUMO than the lighter ones (*ca.*  $\eta = 6.98$  eV for fluorine, 3.05 eV for iodine) with both higher values of the electrophilic grand canonical dual descriptor. Still, these calculations seem to fail to reproduce the rarity of dihalogen-based complexes. In fact, the question is whether this rarity comes from poor coordination abilities or from other causes. As already discussed, the oxidative potential of dihalogens is a quite likely cause of the very few occurrences of dihalogens based complexes. This is the subject of a reactivity study, yet an implicit assumption is that we only consider coordination properties, meaning small perturbations of the electron densities, and not reactivity. Respect to this, our description is correct, and in fact the missing trends can be quite easily found since reactivity can be

attained through a proper (yet slightly different) interpretation of the DD. For instance, the positive regions of the DD indicate acceptor regions in terms of coordination, but also the regions that would induce an electrophilic attack. The difference between the two approaches lies in the considered phenomenon: a slight electron delocalisation (from the metal to the ligand here), or a complete electron transfer (oxidative addition).

### Series (3): from dioxo to peroxo

Isosurfaces for dioxo, superoxo and peroxo ions are represented on figure Figure 3. These ligands are not supposed to show the same reactivity, but they form an electrochemical series that intervenes quite often in bioinorganic chemistry<sup>34</sup> (cell respiration, oxidation cycles).

The differences between all these ligands are striking. The nucleophilicity of dioxo (figure Figure 3 (a),(A)) is essentially located along two orthogonal directions, either along the molecular axis or perpendicular to it. The main development is found in the interatomic plane, which would suggest a chelate mode of coordination, but since the MEP value in this area is positive - it corresponds to the maximum value of *ca.*  $9 \cdot 10^{-3}$  a.u. - this coordination mode is rather disfavoured. In fact, slightly negative values of the MEP are found on the sides of each oxygen atom (*ca.*  $-2 \cdot 10^{-3}$  a.u.), forming circular potential domains at the same places one finds electrophilic parts of the DD. This suggests that dioxygen would essentially bind in a bent side-on way, acting as an acceptor ligand, as depicted on the left side of scheme Scheme 1 (c). Still, coordination by the central nucleophilic area could be encountered when covalent interactions are stronger than electrostatic ones. In such a case dioxo is also expected to be a quite good acceptor ligand. It develops indeed large electrophilic lobes in the vicinity of the coordination area. Eventually, in these two geometries the acceptor tendency could lead to a certain reactivity, as what was formerly discussed for dihalogens. These results seem in a rather good agreement with the known reactivity of dioxo towards complexes: to the best of our knowledge, no dioxygen complex has been yet unambiguously characterised. Indeed, O<sub>2</sub> undergoes in all cases one or several electron back-transfer, e.g. in the haemoglobin

complex<sup>35</sup> where a side-on superoxo is found as sketched on scheme Scheme 1 (c), or in the oxidative addition of O<sub>2</sub> to iridium complexes<sup>36</sup> where usually a chelate peroxo is finally formed. These results are also quite easily understandable in the framework of MO theory. The nucleophilic parts on the molecular axis arise from  $\sigma^*$  contributions, while the central one stems from the bonding  $\pi$  system, which would be stabilised by the approach of an electron-acceptor species. The electrophilic parts are due to the anti-bonding  $\pi^*$  system, which on the contrary would be stabilised by an interaction with an electron-giving species.

Superoxo (figure Figure 3 (b), (B)) shows also a balanced trend since both nucleophilic and electrophilic sites show similar developments. In terms of MO theory, they seem to arise essentially from orthogonal  $\pi^*$  contributions. This suggests that superoxo would be a fairly good donor ligand, with a possibility to show chelation, and some slight abilities for back-bonding due to the development of electrophilic areas in the vicinity of the bonding region. MEP in this case shows only negative values, due to the negative charge of the ligand. Hence, electrostatic interaction is any case stabilising, but it still makes sense to check for the local minima in order to have a better idea of the regioselectivity of a cation approach. The MEP surface in this case was then represented between its minimal and maximal values. It is plain to see that two potential wells are defined above and below the O-O bond, but not in a circular shape (*ca.*  $-0.28$  a.u.). It is worth noticing that the nucleophilic parts of the DD are also located below and above the O-O bond. Both descriptors thus strongly comfort the hypothesis of a chelating, donor superoxo. Little back-bonding is expected in this geometry, as the only reachable electrophilic parts are the ones located in the middle of the O-O bond. Yet, as formerly said the electrostatic interaction is stabilising at any point on the isodensity surface. Situations where stabilisation due to orbital interaction would take precedence over electrostatic interaction are therefore possible. For instance, the displacement of a ligand could increase the back-bonding or the  $\sigma$ -bonding while decreasing the electrostatic stabilisation. Depending on the balance between both effects, this displacement will be favoured or not. As a result, geometries involving a cation not

exactly located in the potential well, but rather on one of its sides, could be encountered. This is also in a good agreement with the known reactivity of superoxo; for instance, as already discussed in the haemoglobin complex  $O_2^-$  binds in a bent-side on form to Fe(III) (yielding a strong  $\sigma$ -donation).

In the case of peroxo (figure Figure 3 (c),(C)) finally, the DD representation is very close to what was seen for fluorine. This was expected since they are isoelectronic. The same kind of reactivity is therefore expected at the DD level: chelate or bent donor, or linear and acceptor ligand. Since peroxo is a dianion, here also one expects to observe only negative values of the potential, hence suggesting to use the same representation (between min and max values). Again, the minimal values are found within the bond area, but this time the potential domain is circular (continuum of minimal values, *ca.* -0.54 a.u.). Chelate mode of coordination is then strongly supported, even if any cation approach is favoured with respect to the MEP (negative values). In this bonding mode, little back-bonding might occur thanks to the central electrophilic developments of the DD, in the middle of the O-O bond. In that case indeed, the O-O bond length is quite long (*ca.* 1.62Å) and the MEP is strongly negative, hence permitting a close approach of a cation and a subsequent strong interaction with this electrophilic part.

All these tendencies are also in a good agreement with the known reactivity of peroxo as a ligand. For instance, in the catechol-oxidase complex, dioxo first binds to two copper(I) ions and then undergoes two electrons back-transfer, yielding peroxo bound to two copper(II) in a chelate way as shown on scheme Scheme 1 (d) and (e). This complex can then oxidise organic molecules such as phenols<sup>34</sup>, hence exploiting the relative electrophilicity of peroxo (middle-bond developments). As previously said for peroxo, here also other geometries are possible since the MEP is attracting towards cations anywhere on the surface. This allows to understand the geometry of  $[(Cu(TMPA))_2(O_2)]^{2+}$  complex, where a peroxo bridges to copper(II) in a end-to-end, bent fashion (cf scheme Scheme 1)<sup>37</sup>. In this case indeed, the chelate binding mode seems disfavoured due to steric hindrance generated by the pyridine

coordinating groups. Another possible way to bind the metallic cations through the donor parts of peroxo is to bridge by a bis-monohapto mode ( $\eta^1 - \eta^1$ ), as experimentally observed. In these cases also, the combination of both the DD and the MEP allows to retrieve the coordination chemistry and also the reactivity of  $O_2$  based complexes.

### Series (4): nitrosyl, carbonyl, cyanide

As previously stated, the ligands in series (4) are isoelectronic and it is well established that they show similar coordination abilities. For instance, carbonyl, cyanide and nitrosyl are known to yield roughly the same kind of crystal field energy splitting, meaning they show the same kind of donor and acceptor abilities<sup>1</sup>. DD and MEP isosurfaces are represented on figure Figure 4. DD displays similar features: nucleophilic domains are found along the molecular axes, pointing outwards the molecule. They are more developed on the most electropositive atom, which is known to be the coordinating one (C in CO, N in  $NO^+$ , C in  $CN^-$ ), and can be understood in the framework of the MO theory as arising from  $\sigma^*$  orbitals. These nucleophilic contributions point on the direction of the minima of MEP ( $-2.10^{-2}$  a.u. for C in CO,  $-0.24$  a.u. for C in  $CN^-$ ,  $0.24$  a.u. for N in  $NO^+$ ), strongly supporting linear coordination mode (with a donor ligand). The development of electrophilic domains in the vicinity of this coordination area (essentially  $\pi^*$  like) indicates a strong tendency towards back-bonding. This is consistent with the fact that these ligands are known to be strong field ligands, with the following order within the spectrochemical series<sup>2</sup>:  $NO^+ < CO \approx CN^-$ . The order within this serie is furthermore retrieved from the spatial extent of the DD, being larger for carbonyl and cyanide as compared to nitrosyl. This is also plain from the condensed values of the grand canonical DD, as reported in table Table 2:  $NO^+$  shows lower contributions (*ca.*  $\pm 3.2$  a.u) than CO (*ca.*  $\pm 4.4$  a.u) and cyanide (*ca.*  $\pm 5.1$  a.u).

In the case of cyanide and carbonyl, the minimal values of the MEP found on the coordinating atom correspond to genuine potential wells; the interplay between charge and covalent interaction therefore suggests that the coordination will essentially imply a linear



Table 2: Condensed grand canonical dual descriptor for CO, NO<sup>+</sup> and CN<sup>-</sup>, sorted by positive or negative contribution.

Molecule	$\Delta f_D^+/\eta^2(\text{a.u.})$	$\Delta f_D^-/\eta^2(\text{a.u.})$
CN <sup>-</sup>	5.06	-5.07
CO	4.37	-4.38
NO <sup>+</sup>	3.17	-3.18

donor ligand, with a large back-bonding, as observed. In the case of cyanide, since the MEP is negative everywhere, coordination by the N atom is also plausible, even though coordination by the C atom is preferred. This accounts quite well for the observed coordination trends of cyanide, noticeably the possibility to form C,N (end-to-end) bridges like in the prussian blue analogues<sup>38</sup>. In these compounds, the large back-bonding manifests itself in the generally large magnetic coupling between the cations. In the case of carbonyl, the relative strength of charge interaction is expected to be lower than what is observed in cyanide, hence suggesting that the restriction to the linear coordination might be weaker, accounting for the possibility to obtain the bent-carbonyl complex carboxyhaemoglobin<sup>39</sup>. This last example is further explained if one remembers that iron in haeme complex is rather nucleophilic (as illustrated by the back-transfer in oxyhaemoglobin between Fe(II) and dioxo), hence trying to increase its interaction with the electrophilic parts of the DD and therefore coordinating in a bent fashion. Finally, in the case of nitrosyl, since no negative MEP value is found, the minimal value corresponds to a repulsive potential (towards cations). As a result, charge control alone limits any coordination (effect of the positive charge). No real interplay between charge and orbital control can be found, and the reactivity must then be controlled solely by orbital interactions. This accounts quite well for the variety of behaviours that nitrosyl can show: when reacting with a quite nucleophilic metal, it will essentially behave like an acceptor in a bent "side-on" geometry<sup>2</sup>, as in  $[\text{Ir}(\text{PPh}_3)_2(\text{CO})(\text{NO})\text{Cl}]^+$ . On the contrary, when reacting with an electrophilic metal, it would behave like a linear donor<sup>40</sup>, as in  $[\text{Fe}(\text{CN})_5\text{NO}]^-$ , with a large tendency to back-bonding.

## Nitrosyl

In the previous series, we discussed a few results for  $\text{NO}^+$ , which is one of the limit forms that one usually writes to describe the behaviour of a one-electron donor nitrosyl ligand. NO is indeed a non-innocent ligand, and its electronic state is almost never plain<sup>41</sup>: it always balances between  $\text{NO}^+$  and  $\text{NO}^-$ . The cationic form might not be the best form to describe NO, especially when aiming to describe its reactivity. Indeed, the positive charge results in an electrostatic repulsion that might forbid complexation. Lets now focus on the neutral, radicalar form  $\text{NO}\cdot$ . Computations of the DD and the MEP are shown in figure Figure 5. Again, both electrophilic and nucleophilic contributions to the dual descriptor are spatially developed, and might be of similar importance for the reactivity. Yet, the differences with the cationic form are marked: instead of planar electrophilic and nucleophilic parts, orthogonal  $\pi^*$ -like contributions are observed. They are mainly located on the N, suggesting a coordination by the nitrogen. This is supported by MEP analysis, showing two local minima on the sides of the N atom (*ca.*  $-12.10^{-3}$  a.u.), to be compared with the local minima on the sides of the O (*ca.*  $-8.10^{-3}$  a.u.). These features are localised on the same places as the nucleophilic parts of the DD, hence suggesting two possible coordination geometries: either bent and donor, with a slight tendency towards back bonding thanks to electrophilic areas not far from the coordination area, or linear and strongly donor ( $\pi$ -donation) with a larger tendency towards back-bonding. This linear form is possible since along the molecular axis the MEP values are negative, hence stabilising for a cation (balance between the full electrostatic stabilisation and the back-bonding). The bent geometry is therefore expected when NO binds to a quite nucleophilic metal, which is consistent with the known data on nitrosyl: the bent form is associated with a 1e donor character while the linear form is associated with a 3e donor character<sup>41</sup>. This is also seen in the Feltham-Enemark model<sup>42</sup>: the more the {MNO} entity contains electrons, the more bent the nitrosyl would be.

Yet, something might seem odd to the reader, since this analysis is in a partial contradiction with the former one on the cationic form: here, the bent geometry is associated

with a donor character, while for the cationic form it is related to an acceptor ability. This is actually consistent with the known "non-innocent" character of nitrosyl as a ligand, and the fundamental ambiguity that stems from the arbitrary assignment of an electronic state to it. Indeed, instead of considering an acceptor nitrosyl and a donor iridium(I) ion in  $[\text{Ir}(\text{PPh}_3)_2(\text{CO})(\text{NO})\text{Cl}]^+$ , one might have thought of a donor nitrosyl bound to an acceptor iridium(II); the apparent problem is only a matter of electron localisation, which should not be encountered while considering entire complexes in which the electronic state of nitrosyl is not relevant (but the total number of electrons is).

## Thiocyanate

Thiocyanate is another example of ambidentate ligand, characterised by the so-called geometry signatures<sup>41</sup>: thiocyanate coordinates by the N atom to hard metals, in a linear geometry, or by the S atom to soft metals, in a rather bent-side on geometry<sup>43</sup>. The MEP and DD maps are displayed in figure Figure 6. One must bear in mind that a proper quantum calculation of sulfur-containing compound supposes the inclusion of diffuse and polarisation functions, thus suggesting the use of 6-31+G\* basis set in this case. From the DD analysis, it seems that the N atom is essentially nucleophilic, while the sulfur atom shows both components. The nucleophilic parts can be viewed as arising from essentially  $\pi^*$ -like orbital (in the framework of MO theory), with a hint of  $\sigma$  character for the nitrogen atom, and the largest component is found on the sulfur. This suggests that both atoms are able to act as donor ligand, with essentially no back-bonding while coordinating by the nitrogen, and on the contrary a possible back-bonding when coordinating by the sulfur in a bent fashion. MEP also shows that any coordination is possible, since at the chosen isodensity all the values are negative. Yet, the minimal value is found along the SCN bond on the nitrogen (*ca.* -0.20 a.u.), and the maximal value is found along the bond but on the S atom (*ca.* -0.15 a.u.).

As a result, one expects hard metals to coordinate by the N atom since they are most

likely to undergo charge control, while on the contrary soft metals, likely to undergo covalent control, would rather bind to the sulfur since it shows the largest nucleophilic contribution and also the possibility to yield back-bonding. In the case of a N-bonding, the geometry is expected to be linear (orientation along the minimal MEP value, along the bond). The S-bonded complexes are expected to be bent because of the better back-bonding (with respect to a linear situation) and at the same time a larger electrostatic interaction. The coordination properties of thiocyanate are here very well reproduced.

### Acetylacetonate and hexafluoroacetylacetonate

Acetylacetonate (acac) is widely used in coordination chemistry, acting as a donor but also quite efficient in enhancing the Lewis acidity of metallic cations, which supposes a quite good attractor behaviour; its hexafluorinated counterpart (hfac) shows the same reactivity, with a larger Lewis acidity enhancement<sup>44</sup>. The computed MEP and DD surfaces are represented on figure Figure 7. It is plain to see that both descriptors indicate a coordination by the two oxygen atoms, preferentially in the molecular plane: the nucleophilic parts of the DD consist essentially of the p-type lone pairs of the oxygens, lying in the molecular plane. On the other hand, a (negative) electrostatic potential well is located between the two oxygens, in the same position (*ca.*  $-0.23$  a.u. for hfac,  $-0.28$  a.u. for acac), while other parts of the molecules show positive values of the MEP (which suggests the charge is quite localised within the two oxygens). One would then expect a quite strong donor character for these ligands, as it is generally observed experimentally. But one can also see that the electrophilic part of the DD, though mostly located on the carbonyl carbons, also develops on the oxygens, perpendicular to the molecular plane. These electrophilic areas are in an appropriate place to allow a quite efficient back-bonding from metal orbitals, thus enhancing its Lewis acidity. This is also experimentally observed. The difference between the protonated and fluorinated form is not really obvious, except that hfac is expected to be a weaker ligand, since MEP minimum is smaller and DD spatial extent is smaller. The MEP feature is quite easily explained if

one remembers that trifluoromethyl groups are electron withdrawing, hence delocalising the anionic density over the whole molecule and not only between oxygens. A more careful look at the DD reveals that the electrophilic and nucleophilic parts are rather comparable for hfac, in contrast to the situation of acac where the nucleophilicity is preponderant. This is likely due to the trifluoromethyl groups, which by lowering the density leads to lower the local nucleophilicity and also the local electrophilicity. As a result, hfac is expected to be a stronger electron-withdrawing ligand as compared to acac, which is consistent with its higher "lewis acidity enhancement" properties<sup>44</sup>.

## 4-Conclusion

In this article, we have shown that the computation of the dual descriptor and the molecular electrostatic potential allows to interpret the coordination chemistry of ligands in terms of acceptor/donor abilities balanced by electrostatic interactions. The variety of the chosen examples (ranging from neutral diatomic to charged polyatomic ligands) supports the generality of the proposed method, not only for geometry interpretation but also its prediction. In many cases, both descriptors provide similar information, but in some cases ambiguities could only be relieved by the combination of the two descriptions. For instance, in the cases of dioxygen (coordination by the electrophilic part of the ligand thanks to the molecular potential) or thiocyanate (coordination possible on every position according to the MEP, limitation to two possibilities thanks to the DD). This tool might be useful for the community of coordination chemists, since it allows to map unambiguously and at the price of rather simple DFT calculations the relative local nucleophilicity or electrophilicity of a ligand, hence permitting to predict the preferential coordination geometries of a given ligand. Furthermore, the effectiveness of the proposed method suggests that it could be worth to check if any complementary informations would not be obtained by considering the dual potential<sup>45,46</sup> instead of the dual descriptor. Yet, the combination of both DD and MEP

already allowed us to get an insight in the electronic properties of a ligand, enabling for instance to ascertain which geometries would allow back-bonding and which ones would not. Furthermore, the scope is not limited to these points. Previous studies showed indeed that charge-transfer excitations could be easily computed and explained basing on the variations of the density upon a vertical excitation<sup>47</sup>, which are precisely what one computes when looking for the state-specific DD<sup>48</sup>. This means that one can access, in a single and unified framework, to both reactivity and optical properties of a molecule, and at a relatively low computational cost.

## Acknowledgements

The authors would like to thank Roald Hoffmann for his precious advice and discussions. F.G. is grateful to the Ecole Normale Supérieure de Lyon for the financial support. This work has been partially supported by INSA Rouen, Rouen University, CNRS, Labex SynOrg (ANR-11-LABX-0029) and region Haute-Normandie (CRUNCH network). L. J. and V. T. thank the Centre National de la Recherche Scientifique (CNRS) for a "chaire d'excellence" at the University of Rouen, and the Centre de Ressources Informatiques de Haute-Normandie (CRIHAN) for computational resources.

## References

- [1] Shriver, D. F.; Atkins, P. W. *Inorganic Chemistry, 3rd edition*; Oxford University Press, 1999.
- [2] Huheey, J. E. *Inorganic Chemistry: Principles of Structure and Reactivity*; Harper International Edition, 1972.
- [3] Chatt, J.; Duncanson, L. A.; Venanzi, L. M. *Journal of the Chemical Society* **1955**, 4456–4460.
- [4] Klopman, G. *Journal of the American Chemical Society* **1968**, *90*, 223–234.
- [5] Salem, L. *Journal of the American Chemical Society* **1968**, *90*, 543–552.
- [6] Morell, C.; Grand, A.; Toro-Labbé, A. *The Journal of Physical Chemistry A* **2005**, *109*, 205–212.
- [7] Morell, C.; Grand, A.; Alejandro, T.-L. *Chemical Physics Letters* **2006**, *425*, 342–346.
- [8] Martinez-Araya, J. *Journal of Molecular Modeling* **2013**, *19*, 2715–2722.
- [9] Pinter, B.; Nagels, N.; Herrebout, W. A.; De Proft, F. *Chemistry - A European Journal* **2013**, *19*, 519–530.
- [10] Cárdenas, C.; Rabi, N.; Ayers, P. W.; Morell, C.; Jaramillo, P.; Fuentealba, P. *The Journal of Physical Chemistry A* **2009**, *113*, 8660–8667.
- [11] Morell, C.; Ayers, P. W.; Grand, A.; Gutierrez-Oliva, S.; Toro-Labbé, A. *Physical Chemistry Chemical Physics* **2008**, *10*, 7239–7246.
- [12] Tognetti, V.; Morell, C.; Ayers, P. W.; Joubert, L.; Chermette, H. *Physical Chemistry Chemical Physics* **2013**, *15*, 14465–14475.
- [13] Zope, R. R.; Baruah, T.; Pederson, M. R.; Dunlap, B. I. *International Journal of Quantum Chemistry* **2008**, *108*, 307–317.

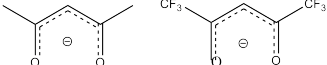
- [14] Jouanno, L.-A.; Di Mascio, V.; Tognetti, V.; Joubert, L.; Sabot, C.; Renard, P.-Y. *The Journal of Organic Chemistry* **2014**, *79*, 1303–1319.
- [15] Geerlings, P.; De Proft, F.; Langenaeker, W. *Chemical Reviews* **2003**, *103*, 1793–1874.
- [16] Morell, C.; Grand, A.; Toro-Labbé, A.; Chermette, H. *Journal of Molecular Modeling* **2013**, *19*, 2893–2900.
- [17] Wang, W.; Mortier, W. J. *Journal of the American Society* **1986**, *108*, 5708–5711.
- [18] Wah, W. M. *Quantum Chemical Calculations of Sulfur-Rich Compounds in Elemental Sulfur and Sulfur-Rich Compounds II*; Elemental sulfur and sulfur-rich compounds; Springer, 2003.
- [19] Hillier, I.; Saunders, V. *Chemical Physics Letters* **1969**, *4*, 163 – 164.
- [20] Yurieva, A.; Poleschchuk, O.; Filimonov, V. *Journal of Structural Chemistry* **2008**, *49*, 548–552.
- [21] Dennington, R.; Keith, T.; Millam, J. GaussView Version 5. Semichem Inc., Shawnee Mission, KS, 2009.
- [22] Frisch, M. J. et al. Gaussian 09 Revision D.01. Gaussian Inc. Wallingford CT 2009.
- [23] Hoffmann, R. *Accounts of Chemical Research* **1971**, *4*, 1–9.
- [24] Rosch, N.; Hoffmann, R. *Inorganic Chemistry* **1974**, *13*, 2656–2666.
- [25] Vaska, L.; DiLuzio, J. W. *Journal of the American Chemical Society* **1962**, *84*, 679–680.
- [26] Kubas, G. J. *Metal Dihydrogen and  $\sigma$ -Bond Complexes*; Kluwer Academic Publishers, 2002; pp 33–51.
- [27] Rogachev, A. Y.; Hoffmann, R. *Journal of the American Chemical Society* **2013**, *135*, 3262–3275.

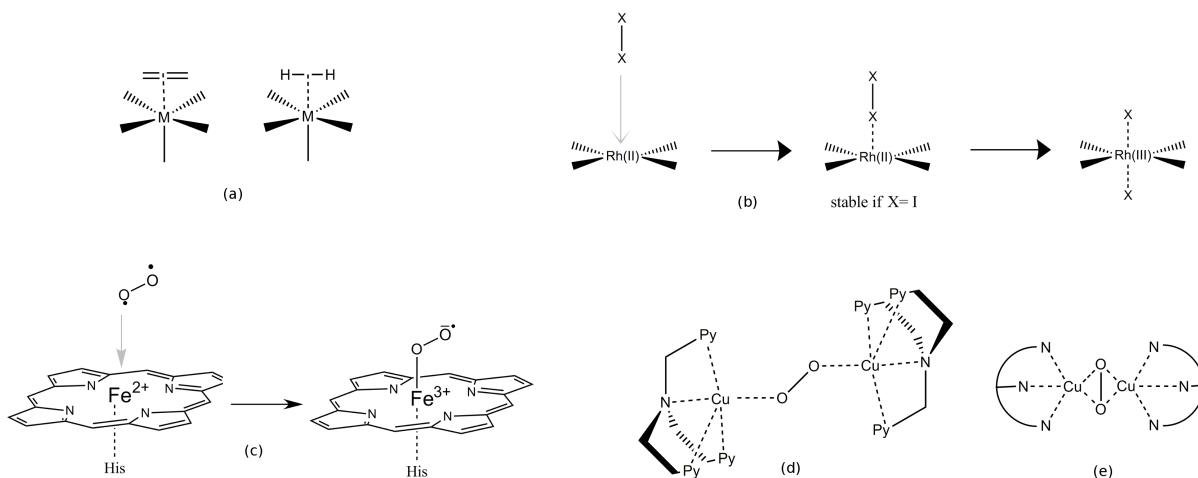


- [28] Gossage, R. A.; Ryabov, A. D.; Spek, A. L.; Stufkens, D. J.; van Beek, J. A. M.; van Eldik, R.; van Koten, G. *Journal of the American Chemical Society* **1999**, *121*, 2488–2497.
- [29] Shaffer, D. W.; Ryken, S. A.; Zarkesh, R. A.; Heyduk, A. F. *Inorganic Chemistry* **2012**, *51*, 12122–12131.
- [30] Makiura, R.; Nagasawa, I.; Kimura, N.; Ishimaru, S.; Kitagawa, H.; Ikeda, R. *Chemical Communications* **2001**, 1642–1643.
- [31] Cotton, F. A.; Dikarev, E. V.; Petrukhina, M. A. *Angewandte Chemie International Edition* **2000**, *39*, 2362–2364.
- [32] Clark, T.; Hennemann, M.; Murray, J.; Politzer, P. *Journal of Molecular Modeling* **2007**, *13*, 291–296.
- [33] Vanýsek, P. *Handbook of Chemistry and Physics: 92nd Edition*; Taylor and Francis Group, 2011; pp 5–80 – 5–89.
- [34] Kitajima, N.; Moro-oka, Y. *Chemical Reviews* **1994**, *94*, 737–757.
- [35] Pin, S.; Alpert, B.; Michalowicz, A. *FEBS Letters* **1982**, *147*, 106 – 110.
- [36] Rybak-Akimova, E. V. *Physical Inorganic Chemistry: Reactions, Processes, and Applications*; Wiley, 2010; pp 109–188.
- [37] Moro-oka, Y.; Fujisawa, K.; Kitajima, N. *Pure & Applied Chemistry* **1995**, *67*, 241–248.
- [38] Verdaguer, M.; Girolami, G. S. *Magnetism: Molecules to Materials V*; Wiley-VCH Verlag, 2005; pp 283–346.
- [39] Vasquez, G. B.; Ji, X.; Fronticelli, C.; Gilliland, G. L. *Acta Crystallographica Section D* **1998**, *54*, 355–366.

- [40] Navaza, A.; Chevrier, G.; Alzari, P. M.; Aymonino, P. J. *Acta Crystallographica Section C* **1989**, *45*, 839–841.
- [41] Mingos, D. P. *Journal of Organometallic Chemistry* **2014**, *751*, 153 – 173.
- [42] Enermark, J. H.; Feltham, R. D. *Coordination Chemistry Reviews* **1974**, *13*, 339–406.
- [43] Kabesova, M.; Gazo, J. *Chemické Zvesti* **1980**, *6*, 800–841.
- [44] Bailey, N. A.; Fenton, D. E.; Franklin, M. V.; Hall, M. *Journal of the Chemical Society, Dalton Transactions* **1980**, 984–990, and references therein.
- [45] Morell, C.; Ayers, P. W.; Grand, A.; Chermette, H. *Physical Chemistry Chemical Physics* **2011**, *13*, 9601–9608.
- [46] Morell, C.; Labet, V.; Ayers, P. W.; Genovese, L.; Grand, A.; Chermette, H. *Journal of Physical Chemistry A* **2011**, *115*, 8032–8040.
- [47] Le Bahers, T.; Adamo, C.; Ciofini, I. *Journal of Chemical Theory and Computation* **2011**, *7*, 2498–2506.
- [48] Syzgantseva, O. A.; Tognetti, V.; Boulangé, A.; Peixoto, P. A.; Leleu, S.; Franck, X.; Joubert, L. *The Journal of Physical Chemistry A* **2014**, *118*, 757–764.

Table 3: Series of studied ligands.

Series number	Ligands
(1)	$H_2, CH_2CH_2$
(2)	$F_2, Cl_2, Br_2, I_2$
(3)	$O_2, O_2^-, O_2^{2-}$
(4)	$NO^+, CO, CN^-$
(5)	$NO\cdot$
(6)	$SCN^-$
(7)	Acetylacetonate, hexafluoro-acetylacetonate 



Scheme 1: Schematic representation of: **(a)**, the  $\eta^2$  coordination mode of ethene (left) and  $H_2$  (right); **(b)**, the reaction of  $[(dpp-nacnac^{CH_3})Rh(phdi)]$  with iodine; **(c)**, the reaction of dioxo with the haeme moiety in haemoglobin; **(d)**, coordination of peroxo in the  $[(Cu(TMPA))_2(O_2)]^{2+}$ ; **(e)**, coordination of peroxo in the catechol oxidase complex

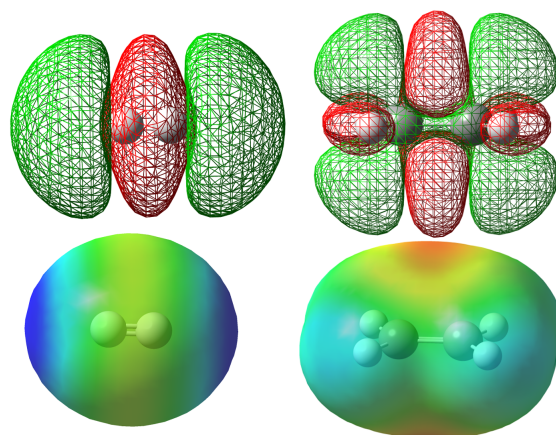


Figure 1: **Up:** DD isosurfaces for  $\text{H}_2$  and ethylene (from left to right). Isovalues:  $\pm 4.10^{-3}$  a.u., green:  $\Delta f > 0$ , red:  $\Delta f < 0$ .

**Down:** MEP maps on density isosurfaces, same order. Isodensity:  $1.10^{-3}$  a.u., values ranging from  $3.00 \cdot 10^{-2}$  (blue) to  $-3.00 \cdot 10^{-2}$  a.u. (red) in the case of ethene,  $1.00 \cdot 10^{-3}$  to  $-1.00 \cdot 10^{-3}$  for  $\text{H}_2$ .

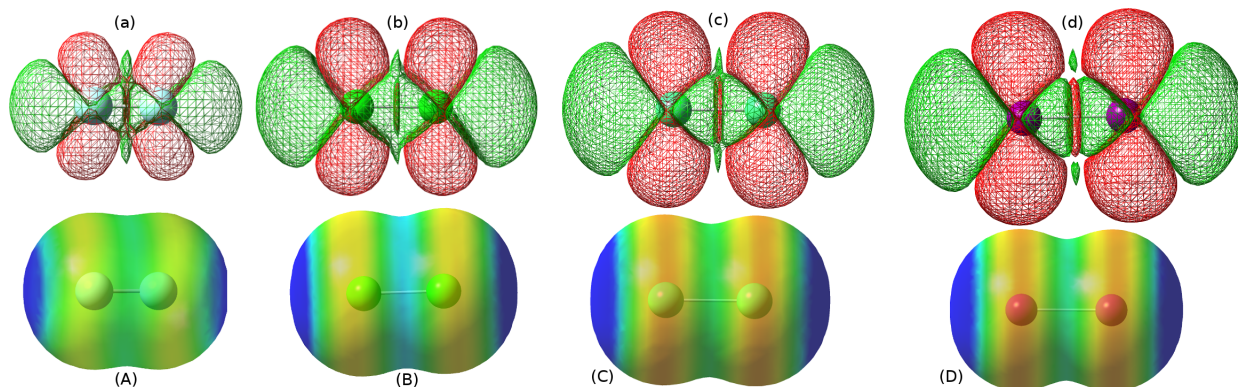


Figure 2: DD isosurfaces (up) and MEP maps on density isosurfaces (down) for the dihalogens from  $\text{F}_2$  (indices **A**) to  $\text{I}_2$  (index **D**). DD isovalues:  $\pm 4.10^{-3}$  a.u., MEP ranges:  $[-1.00 \cdot 10^{-2}; 1.00 \cdot 10^{-2}]$  a.u., same color scheme as figure Figure 1.

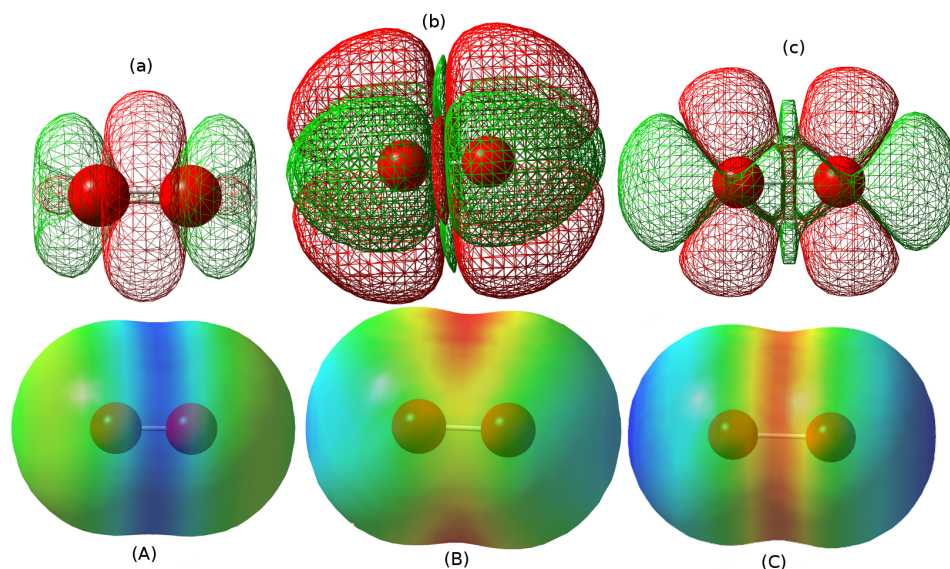


Figure 3: DD isosurfaces (up) and MEP maps on density isosurfaces (down) for  $O_2$ ,  $O_2^-$  and  $O_2^{2-}$  (indices **A**, **B** and **C**). DD isovalues:  $\pm 4.10^{-3}$  a.u., MEP ranges:  $[-1.00 \cdot 10^{-2}; 1.00 \cdot 10^{-2}]$  a.u.,  $[-2.80 \cdot 10^{-1}; -2.30 \cdot 10^{-1}]$  a.u. and  $[-5.50 \cdot 10^{-1}; -4.50 \cdot 10^{-1}]$  a.u. respectively, same color scheme as figure Figure 1.

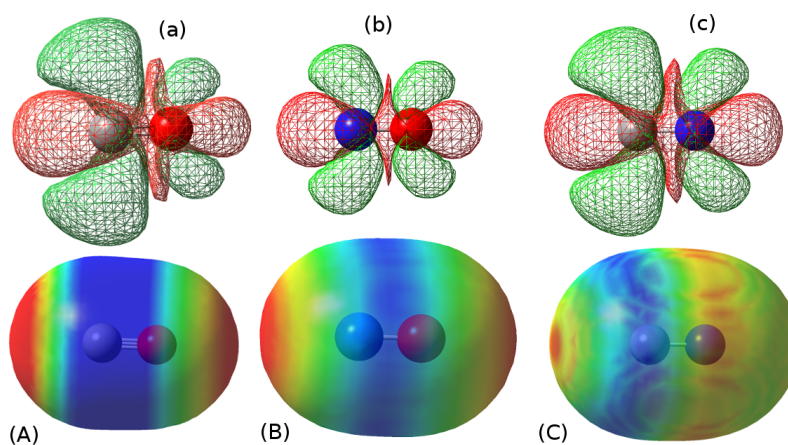


Figure 4: DD isosurfaces (up) and MEP maps on density isosurfaces (down) for  $CO$ ,  $NO^+$  and  $CN^-$  (indices from **A** to **C**). DD isovalues:  $\pm 4.10^{-3}$  a.u., MEP ranges:  $[-2.00 \cdot 10^{-2}; 2.00 \cdot 10^{-2}]$  a.u. ( $CO$ ),  $[2.48 \cdot 10^{-1}; 3.10 \cdot 10^{-1}]$  a.u. ( $NO^+$ ),  $[-2.40 \cdot 10^{-1}; -2.30 \cdot 10^{-1}]$  a.u. ( $CN^-$ ), same color scheme as as figure Figure 1.



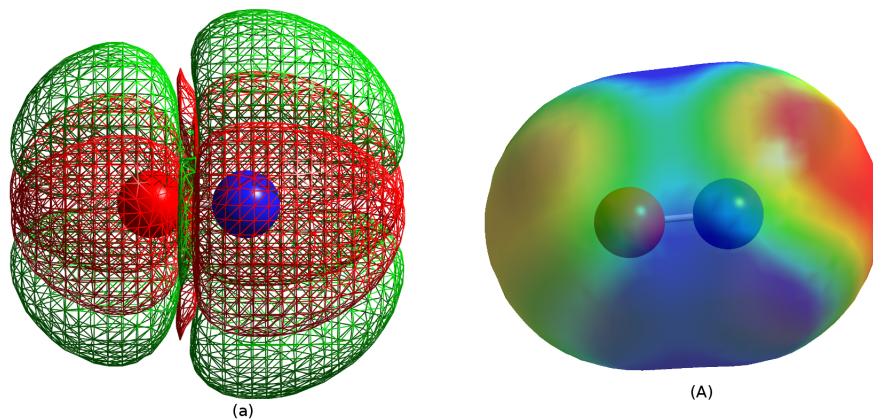


Figure 5: DD isosurface (left) and MEP maps on density isosurfaces (right) for  $\text{NO}\cdot$ . DD isovalues:  $\pm 4 \cdot 10^{-2}$  a.u., MEP range:  $[-1.20 \cdot 10^{-2}; 1.20 \cdot 10^{-2}]$  a.u. Same color scheme as figure Figure 1.

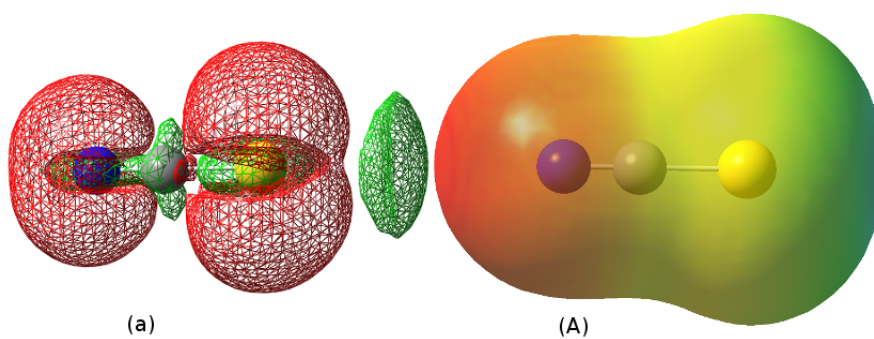


Figure 6: DD isosurface (left) and MEP maps on density isosurfaces (right) for  $\text{SCN}^-$ . DD isovalues:  $\pm 2 \cdot 10^{-2}$  a.u., MEP range:  $[-1.99 \cdot 10^{-1}; -1.50 \cdot 10^{-1}]$  a.u., same color scheme as figure Figure 1.

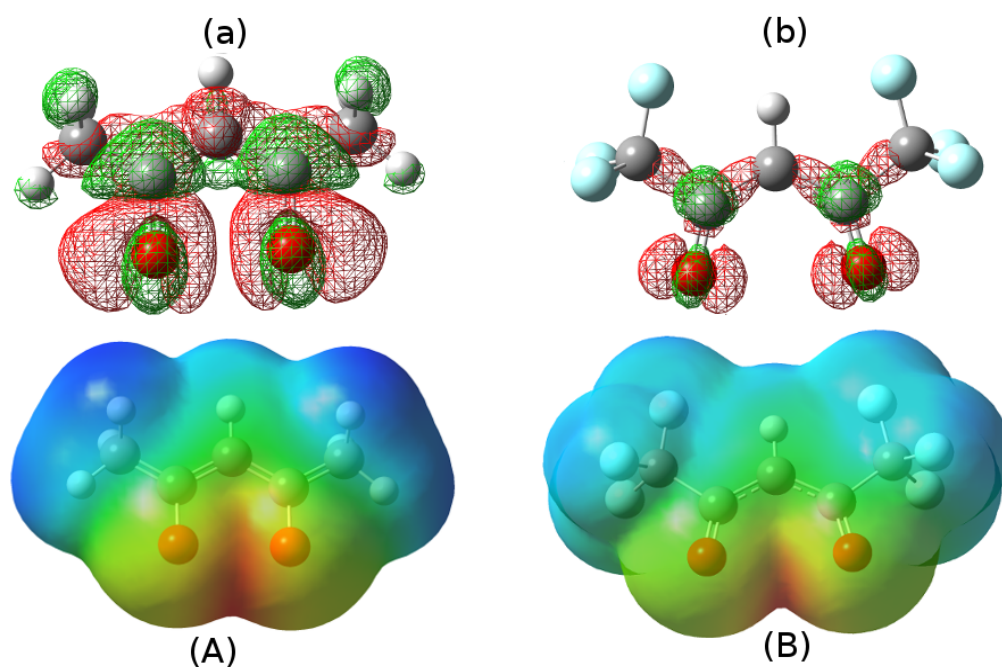


Figure 7: DD isosurface (up) and MEP maps on density isosurfaces (down) for acetylacetonate and hexafluoro-acetylacetonate (indices **A** and **B**). DD isovalues:  $\pm 4.10^{-2}$  a.u., MEP ranges:  $[-2.80 \cdot 10^{-1}; -1.00 \cdot 10^{-1}]$  a.u. (acac),  $[-2.30 \cdot 10^{-1}; -1.00 \cdot 10^{-1}]$  a.u. (hfac), same color scheme as figure Figure 1.



The possibility to retrieve the coordinating properties of ligands by a joined Dual Descriptor and Molecular Electrostatic Potential analysis is shown, yielding a potentially predictive tool towards their ambiphilicity and selectivity.

